Physica Scripta. Vol. 16, 65–69, 1977

Measurements of Optical Lifetimes >1 μs Using Pulsed Electron Excitation Techniques

L. J. Curtis

Department of Physics, University of Lund, Lund, Sweden

P. Erman

Research Institute of Physics, Stockholm, Sweden

Received May 15, 1977

Abstract

Measurements of optical lifetimes >1 μ s using pulsed electron excitation techniques. L. J. Curtis (Department of Physics, University of Lund, Lund, Sweden) and P. Erman (Research Institute of Physics, Stockholm, Sweden). *Physica Scripta (Sweden) 16*, 65–69, 1977.

A study has been made of possible effects which could distort decay curves of atomic and molecular levels with lifetimes >1 μ s when measured using delayed coincidence techniques following pulsed excitation of a static gas cell. Measured decay curves are compared to calculational models, quantitative estimates are established in terms of experimental parameters, and methods for minimizing and correcting these distortions are discussed.

1. Introduction

As is clear from other talks at this conference [1, 2], the use of delayed coincidence techniques following pulsed excitation of a static gas cell is a versatile and reliable method for determining atomic and molecular meanlives in the nanosecond to microsecond range, but the interpretation of these decay curves requires special precautions when the lifetimes studied exceed this range. In such cases the lifetime becomes comparable to the time between intermolecular collisions and to the time required for a molecule to migrate out of the observation region, due either to its thermal motion, or (in the case of charged ions) to the drifts arising from interionic electrostatic repulsion. We have made a semi-empirical study [3] of the possible effects which could distort decay curves of long lived molecular states, in which we have compared measured data with simple calculational models. Our aim was to establish quantitative estimates of the magnitude of these effects in terms of specific experimental parameters, and to devise methods to minimize and correct for their influence on extracted meanlife estimates.

2. Collisional de-excitation and time dependent detection efficiencies

The decay curve of the emitted radiation from a given molecular state n is proportional to its instantaneous population $N_n(t)$, which is governed by the generalized Stern–Volmer equation

$$dN_n/dt = -[1/\tau_n + D_{coll}]\,N_n(t) + Q(t) \tag{1}$$

Here τ_n is the radiative meanlife and D_{coll} is the collisional de-excitation rate, given from the cross section σ_{coll} by

$$D_{coll}(\mu s^{-1}) = 0.0140\, p(\text{mtorr})\, \sigma_{coll}(10^{-16}\,\text{cm}^2)/[T(\text{K})\, M_r(\text{amu})]^{1/2} \tag{2}$$

where p and T are the pressure and temperature of the source gas, and M_r is the reduced mass of the excited-molecule source-gas-molecule binary system. The quantity $Q(t)$ includes all processes exclusive of radiative decay and inelastic collisions between excited and source gas molecules, i.e., the excitation pulse, repopulation due to cascading from higher levels, radiation trapping, excitation transfer between excited molecules, secondary electron interactions, etc. Here we neglect all of these processes except for the excitation pulse, which also vanishes after some finite turn-off time $t=0$. Thus for $t \geqslant 0$ the solution to eq. (1) is

$$N_n(t) = N_n(0) \exp\,[-t/S\tau_n] \tag{3}$$

where S is the Stern–Volmer factor, defined

$$S \equiv 1/(1 + D_{coll} \cdot \tau_n) \tag{4}$$

Thus the *emitted* radiation is a pure exponential, with its functional form independent (except for normalization) of the time since excitation. The 1/e folding time is dependent upon the source conditions through D_{coll}, which can be varied in a controlled way so as to extract τ_n from $S\tau_n$. However, escape of molecules from the viewing volume will introduce a detection efficiency $E(t)$, which depends upon the time since excitation, and can distort the exponentiality of the *detected* radiation. In general the detected radiation involves a convolution of eq. (3) and E at $t-t'$, over the excitation pulse $Q(t')$. We here consider the behaviour of $E(t)$ following impulsive excitation at $t=0$, since the results for any other pulse shape can be obtained by a convolution of this result. With this assumption, the detected radiation is proportional to $\exp(-t/S\tau_n)\,E(t)$, which is non-exponential unless $E(t)$ is a constant or itself an exponential.

Although we have admitted the possibility of gas kinetic collisional effects in de-exciting inelastic collisions, we neglect the effects of elastic collisions which return escaping excited gas molecules to the observation region. This assumption is justified since we consider only free molecules in a low pressure gas cell, with no confining buffer gas. At millitorr pressures the mean free path of an excited molecule passing through the source gas is usually very much larger than the size of the interaction and observation regions, as are the enclosure walls of the gas cell. Thus thermal migration and electrostatic drift from the observation region are non-equilibrium processes, in which particles acquire a spatial distribution which depends upon their own individual velocities and not that characteristic to any temperature reservoir. Therefore our study cannot utilize the more

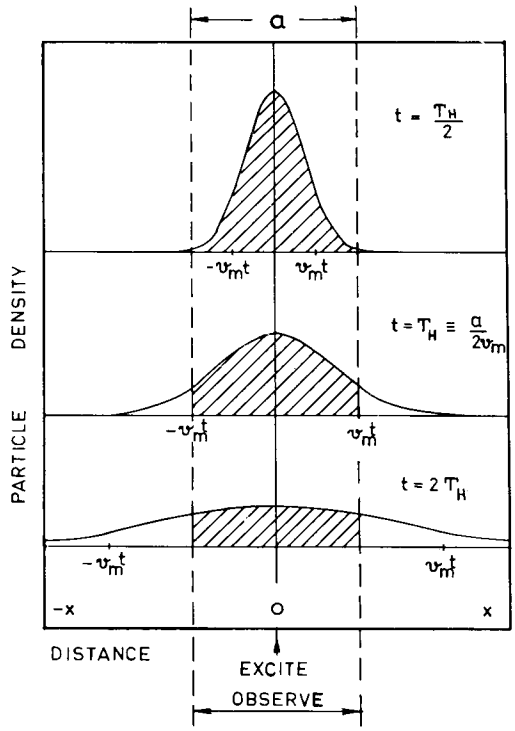

Fig. 1. One dimensional illustration of escape by thermal migration. The distribution of particles in space and velocity (initially localized to $x=0$ with a Maxwellian velocity distribution) is shown at various times after excitation. If only those particles within the region $-a/2<x<a/2$ are observed, the detection efficiency is proportional to the shaded area.

commonly used approach involving thermodynamic macroscopic diffusion equations and coefficients, and must instead consider the kinematics and dynamics of a representative molecule.

3. Thermal migration out of the observation region

We assume a Maxwellian distribution of velocities with most probable speed v_m given by

$$v_m(\mathrm{cm}/\mu\mathrm{s}) = 0.0129[T(\mathrm{K})/M_n(\mathrm{amu})]^{1/2} \tag{5}$$

where M_n is the mass of the excited molecule. We neglect directed velocities due to effusion of the gas into the cell, dissociative recoil, and other similar effects which can only be considered in the context of specific experimental conditions.

If the spatial distribution were initially concentrated along the beam at $t=0$, at any time later the distance from any molecule to the beam axis would be proportional to the velocity of that molecule. (In a microcosmological analog of Hubble's Law, distance and velocity are here proportional.) A one dimensional representation of this process is given in Fig. 1. The Gaussian function which spreads linearly with time represents the distribution of particles in both position and velocity space. As time progresses the faster particles pass out of the observation volume $-a/2 \leqslant x \leqslant a/2$ leaving the slower behind, and the efficiency $E(t)$ is proportional to the shaded area under the curve. It is clear that $E(t)$ will be an S-shaped function, since for small t only a few high speed particles on the distribution tails escape, but this increases until, at large t, only the very slow (and therefore nearly monoenergetic) centre of the distribution remains, which sinks in proportion to the normalization factor $1/t$. This analysis can easily be extended to include an excitation region of finite extent, $-b/2 \leqslant x \leqslant b/2$, and escape in two dimensions, along both the width (a and b) and depth (a' and b') of the beam. This yields

$$E(t) = \prod_{\substack{T_H\,T'_H \\ \varepsilon\;\;\varepsilon'}} \left[1 - \frac{\mathrm{i}^{(1)}\,\mathrm{erfc}\,(\varepsilon T_H/t) - \mathrm{i}^{(1)}\,\mathrm{erfc}\,(T_H/t)}{(1-\varepsilon)(T_H/t)}\right] \tag{6}$$

where $\mathrm{i}^{(1)}\,\mathrm{erfc}\,(Z)$ is the integral of the complementary error function [4] and T_H and ε denote (for the unprimed and primed coordinates along the width and depth of the beam) the geometric parametrizations

$$T_H \equiv (a+b)/2v_m \quad \text{and} \quad \varepsilon \equiv |a-b|/(a+b) \tag{7}$$

A one dimensional projection of eq. (6) (i.e., the bracketed portion of eq. (6), or the entire expression with $T'_H \to \infty$) is plotted in Fig. 2. Its asymptotic properties are given by

$$E(\varepsilon \to 1,\, t < T_H) \to 1 \tag{8}$$

$$E(\varepsilon \to 0,\, t < T_H) \to 1 - t/T_H\sqrt{\pi} \tag{9}$$

$$E(\varepsilon,\, t > T_H) \to (1+\varepsilon)(T_H/t\sqrt{\pi}) \tag{10}$$

Notice that for $t < T_H$ the variation of E with time can be greatly

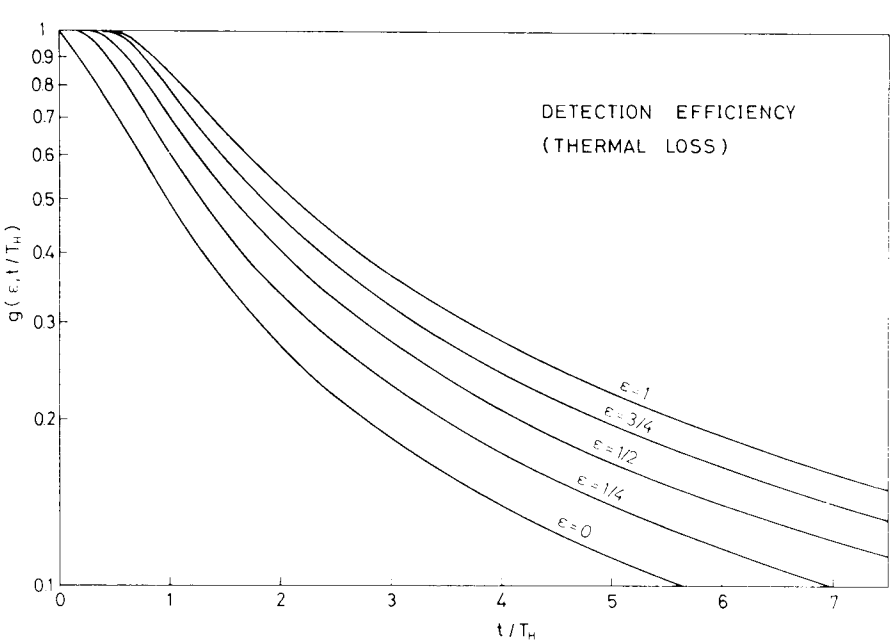

Fig. 2. Detection efficiency for radiation from particles undergoing thermal migration. T_H is a time which characterizes the process and ε parametrizes the relative extent of the excitation and observation regions ($\varepsilon=0$ for congruent excitation and observation region, $\varepsilon=1$ for one much larger than the other). This efficiency is separately computed for the two escape directions perpendicular to the beam, and the total efficiency obtained as their product.

reduced by designing the excitation and observation regions to be very dissimilar in size ($\varepsilon \to 1$). However, for $t < T_H$ E is at worst very nearly an exponential (eq. (9) has the same form as the first two terms of an exponential, although the latter is a somewhat worse approximation to eq. (6)), so $E(t)$ modifies the 1/e folding time but does not distort the basic exponentiality of the detected radiation. For $t > T_H$ the efficiency falls off as $1/t^2$ ($1/t$ for each direction of escape) and long lifetimes could be determined through delayed observations on the slow, nearly monoenergetic remnant after several T_H intervals, which could be efficiency-corrected by multiplying by a factor t^2.

We have tested the predictions of eq. (6) on decay curves of long lived molecular states which exhibit non-exponential curvatures. Our results indicate that these distortions are well described by eq. (6), and this has permitted new measurements of higher precision for the meanlives of these systems.

One such candidate was the Lyman–Birge–Hopfield system in N_2. Our uncorrected measurements showed clear non-exponential curvatures which, if ignored, would infer an effective meanlife of $\simeq 35$ μs. These distortions were only very weakly affected by pressure variations, indicating that inelastic collisions were not a serious de-excitation mechanism. Earlier reported measurements of this meanlife ranged from 5–170 μs. After deconvolution of $E(t)$ from our measured decay curves (the deconvolution was relatively insensitive to the temperature assumed within the source gas, but followed correctly the predicted geometric dependence with a, b, a' and b') the semilogarithmic plot became completely linear, yielding a lifetime of $\tau = 120 \pm 20$ μs.

Another similar example involved the Cameron bands in CO. Here the lifetime was so long (in the millisecond range) that collisional de-excitation was also a problem, which provided an opportunity to test the assumption that inelastic collisional de-excitation can be substantial while elastic collisions which return escaping excited molecules to the observation region are insignificant. We found here that the deconvolution of thermal escape effects completely removed the curvatures on the semilogarithmic plots of the decay curves, and that the 1/e folding time so extracted varied linearly with the pressure of the source gas, in agreement with eqs. (2), (3) and (4). Previously reported measurements ranged from 1–12 milliseconds, and our extrapolations to zero pressure indicated a lifetime $1.5 \pm^{2.1}_{1.5}$ milliseconds.

4. Electrostatic drift out of the observation region

For ion molecules there is also a mutual electrostatic repulsion which, unlike the thermal case, causes an accelerated motion outward from the axis of the beam path. Again using a one dimensional example, we consider an initially uniform sheet of charge distributed within $-b/2 \leqslant x \leqslant b/2$. For an arbitrarily selected ion at a position $X(t)$ within this expanding sheet it can be shown from simple electrostatic considerations that the acceleration, velocity and position are given by

$$\ddot{X}(t)/X(0) = 2/T_c^2 \tag{11}$$

$$\dot{X}(t)/X(0) = 2t/T_c^2 \tag{12}$$

$$X(t)/X(0) = 1 + (t/T_c)^2 \tag{13}$$

with the characteristic time T_c defined as

$$T_c(\mu s) \equiv 1\,070\,[M_n(\text{amu})/\varrho_0(\text{ions/cm}^3)]^{1/2} \tag{14}$$

where ϱ_0 is the initial charge density. Eq. (13) clearly shows that,

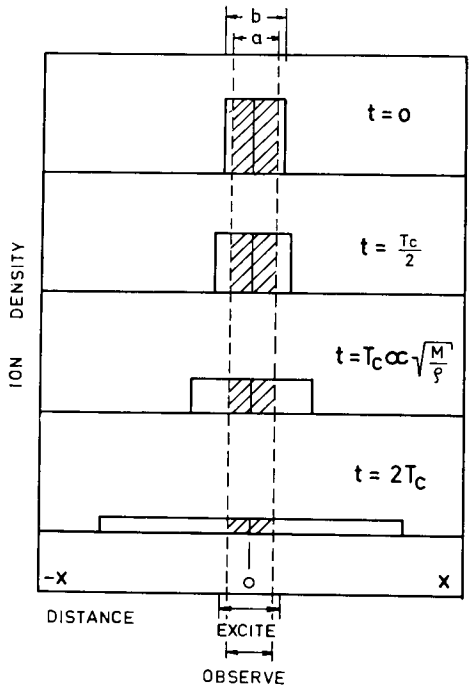

Fig. 3. One dimensional illustration of escape by electrostatic drift. Initially all ions are in the region $-b/2 \leqslant x \leqslant b/2$, but only those within $-a/2 \leqslant x \leqslant a/2$ are under observation. At successive times the distribution expands, and the detection efficiency is proportional to the shaded area.

since the positions of all ions scale with their initial positions, the distribution will remain homogeneous throughout the expansion, with the instantaneous charge density proportional to $X(0)/X(t)$. The situation is illustrated in Fig. 3. If the region $-a/2 \leqslant x \leqslant a/2$ is under observation the efficiency will be given by the shaded area in Fig. 3, which is proportional to the reciprocal of eq. (13) (unless $a > b$, in which the efficiency will remain constant until the distribution expands to fill the field of view, after which it too decreases in proportion to the reciprocal of eq. (13)). This treatment can easily be extended to two dimensions by consideration of an initially uniform cylinder of charge along the beam, and setting $E(t)$ equal to the ratio of its initial volume to that after some expansion time, which yields

$$t/T_c = (\pi/2)^{1/2}\text{erfi}\,([\ln (E)^{-1/2}]^{1/2}) \tag{15}$$

which can be inverted using tabulations of the imaginary error function erfi(Z) [4] or by a novel expansion of this function [3]. The latter approach yields

$$E(t) \simeq [1 + (2/\pi)(t/T_c)^2]^{-\pi/2} \tag{16}$$

Fig. 4 shows the numerical inversion of eq. (15) (solid curve) together with the approximation of eq. (16). The asymptotic forms of eq. (15) can also be inverted to give

$$E(t < T_H) \to \exp(-t^2/T_c^2) \tag{17}$$

$$E(t > T_H) \to [(t/T_c)^2 \ln (t/T_c)^2]^{-1} \tag{18}$$

Although Figs. 2 and 4 look superficially very similar, their behaviour for times short relative to the characteristic times are quite different. Comparison of eq. (17) to eqs. (8) and (9) shows that, unlike the thermal migration, the electrostatic drift will, even for short times, introduce a parabolic curvature into the semilogarithmic plot of the decay curve which will render meaningless the concept of a 1/e folding time. For large t the thermal migration and electrostatic drift efficiencies become quite similar,

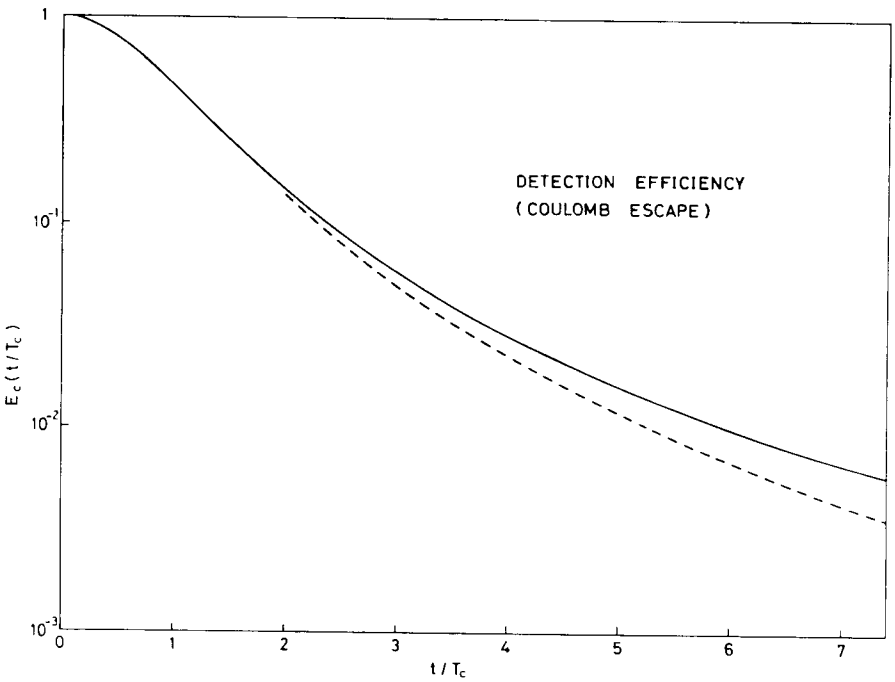

Fig. 4. Detection efficiency for radiation from particles undergoing electrostatic drift. T_c is a time which characterizes the process. A cylindrical geometry is assumed. The solid line indicates the numerical solution, while the dashed line denotes a simple algebraic approximation formula.

with eq. (18) having a small logarithmic distortion to the $1/t^2$ power law of the two dimensional case of eq. (10).

The separation of the detection efficiency from the collisional effects is not as simple in the electrostatic drift case as it was in the thermal migration case, since here both D_{coll} and T_c depend upon the source gas pressure. The pressure dependence of T_c arises through ϱ_0, and is complicated by the fact that it contains two components

$$\varrho_0 = \varrho_0^+ - \varrho_0^- \tag{19}$$

where ϱ_0^+ is charge produced by the excitation pulse, and is calculable from

$$\varrho_0^+(\text{ions/cm}^3) = (6.03 \times 10^9) \times \frac{p(\text{mtorr})\, i(\text{ma})\, \Gamma(\mu s)\, \sigma_{\text{ion}}(10^{-16}\,\text{cm}^2)}{T(\text{K})\, A(\text{cm}^2)} \tag{20}$$

Here i is the average beam current during a pulse of effective length Γ, σ_{ion} is the total cross section for all ionization processes and A is the cross sectional area of the beam. The quantity ϱ_0^- represents the density of electrons which are in the environment, and their contribution is much more difficult to assess. It is very sensitive to experimental parameters and can vary greatly with experimental geometry and operating conditions, making comparisons between different experimental measurements very difficult. However, even if ϱ_0^- cannot be independently determined, eq. (16) can still be used to correct charge affected decay curves, since they can be non linear least squares fitted to the function

$$I(t) = C[1 + (2/\pi)(t/T_c)^2]^{-\pi/2} \exp(-t/S\tau_n) \tag{21}$$

where C, T_c and $S\tau_n$ are all fitting parameters. This determines not only the effective lifetime $S\tau_n$, but also ϱ_0^- by virtue of eqs. (14), (19) and (20). We have tested this for several charge affected decay curves, and have found that eq. (21) describes such curves quite well. However, the extraction of τ_n from $S\tau_n$ is difficult, owing to the pressure dependences of eqs. (2), (4) and (20), and to obtain high reliability in values of τ_n we have sought an alternative method for circumventing these charge effects.

Although the difficulties in estimating ϱ_0^- complicate the calculational modeling of the electrostatic drift, its contribution to the charge distribution is very beneficial for the measurement of meanlives. If experimental conditions are such that $\varrho_0^- = \varrho_0^+$ all charge effects should disappear. The presence of low velocity electrons among the positive ions should not affect their excitation or ionization. Both the number of electrons involved and the cross sections for ionization and excitation are down by orders of magnitude relative to those appropriate to the conditions of the excitation pulse, and recombination times are very long on this scale. Thus we have developed a technique [3] whereby we can control ϱ_0^- through a secondary source of low energy electrons injected into the excitation region. As this neutralizing current is gradually turned up the charge distortions can be seen to diminish, until complete neutralization is obtained. After this point the neutralization is retained, since overcompensation is space charge limiting and therefore self regulating. Thus complete neutralization is signaled by stability of the decay curve under further increases in neutralizing current. This technique has already revealed a number of cases where older measurements were in error by factors of 2–3 due to these charge effects, and new values for lifetimes have been reported in OH^+ [3], H_2O^+ [3], CH^+ [5] and O_2^+ [6].

Conclusions

Our results indicate that the distortion effects introduced into pulsed excitation delayed coincidence measurements by thermal migration and electrostatic drift can be satisfactorily described by simple models, and these effects corrected or eliminated through appropriate measures. Thus the advantages of this method can be utilized in the measurement of lifetimes substantially longer than one microsecond. In closing we note one disappointing result of our analysis. It has been pointed out that there are certain cases where the theoretical assumptions which are used to deduce the exponential law break down, and the radiative decay law should, for large t, approach an inverse power law t^{-m}, where m is a number determined by the specific decay model (cf. refs. [7], [8] and the earlier references cited

therein). Examination of eqs. (10) and (18) indicates the problems which thermal migration and electrostatic drift would pose if these techniques were utilized in a search for such effects.

References

1. Erman, P., Physica Scripta (Lund Conference on Atomic and Molecular Transition Probabilities).
2. Möhlmann, G. R. and de Heer, F. J., Physica Scripta (Lund Conference on Atomic and Molecular Transition Probabilities).
3. Curtis, L. J. and Erman, P., J. Opt. Soc. Am. (in press).
4. Abramowitz, M. and Stegun, I. A., "Handbook of Mathematical Functions" (NBS Appl. Math. Series 55, Washington, D.C. 1970).
5. Erman, P., Astrophys. J. **213**, L89 (1977).
6. Erman, P. and Larsson, M., Physica Scripta **15**, 335 (1977).
7. Nicolaides, C. A. and Beck, D. R., Phys. Rev. Lett. **38**, 683 (1977).
8. Knight, P. L., Phys. Lett. **61A**, 25 (1977).

Department of Physics
University of Lund
Sölvegatan 14
S-223 62 Lund
Sweden

Research Institute of Physics
Roslagsvägen 100
S-104 05 Stockholm
Sweden